The microbiota of breast tissue and its association with tumours

Camilla Urbaniak[1,2], Gregory B. Gloor[3], Muriel Brackstone[4], Leslie Scott[4], Mark Tangney[5] and Gregor Reid[1,2,#]

Affiliations:

[1]Lawson Health Research Institute, London, ON, N6A 4V2, Canada

[2]Department of Microbiology &Immunology, Western University, London, ON, N6A 5C1, Canada

[3] Department of Biochemistry, Western University, London, ON, N6A 5C1, Canada

[4] London Regional Cancer Program, London, Ontario, N6A 4L6, Canada

[5]Cork Cancer Research Centre, University College Cork, Cork, Ireland

Corresponding author: Gregor Reid, Lawson Health Research Institute, 268 Grosvenor Street, London, Ontario, Canada, N6A 4V2. e-mail: gregor@uwo.ca. Tel: 519-646-6100 x65256. Fax:519-646-6031

Key words: breast tissue microbiota, 16S rRNA amplicon sequencing, breast cancer, DNA damage

Conflict of interest: The authors declare no competing financial interests

Abstract: In the United States, 1 in 8 women will be diagnosed with breast cancer in her lifetime. Along with genetics, the environment also contributes to disease development but what these exact environmental factors are remain unknown. We have previously shown that breast tissue is not sterile but contains a diverse population of bacteria. We thus believe that the host's local microbiome could be modulating the risk of breast cancer development. Using 16S rRNA amplicon sequencing we show that bacterial profiles differ between normal adjacent tissue from women with breast cancer and tissue from healthy controls. Women with breast cancer had higher relative abundances of *Bacillus*, *Enterobacteriaceae* and *Staphylococcus*. *Escherichia coli* (member of the *Enterobacteriaceae* family) and *Staphylococcus epidermidis,* isolated from breast cancer patients, were shown to induce DNA double stranded breaks in HeLa cells using the γH2AX assay. We also found that microbial profiles are similar between normal adjacent tissue and tissue sampled directly from the tumour. This novel study raises important questions as to what role the breast microbiome plays in disease development or progression and how we can manipulate this microbiome for possible therapeutics or prevention.

Statement of significance: This study shows that different bacterial profiles in breast tissue exist between healthy women and those with breast cancer. Higher relative abundances of bacteria, that had the ability to cause DNA damage *in vitro*, were detected in breast cancer patients, as well as a decrease in some lactic acid bacteria, known for their beneficial health effects, including anti-carcinogenic properties. This study raises the important question as to the role of the mammary microbiome in modulating the risk of breast cancer development.

52 **Introduction**

53 Bacteria inhabit numerous body sites and this collection of bacteria, termed the human
54 microbiota, plays an integral role in human development. Changes in the composition of one's
55 microbiota, at various body sites, could promote disease progression, as individuals with
56 periodontitis (1)(2), inflammatory bowel disease (3), psoriasis (4), asthma (5), diabetes (6),
57 bacterial vaginosis (7) and colorectal cancer (8) have different bacterial communities compared
58 with healthy individuals. While it is still unclear whether these microbial differences are a
59 consequence or a cause of the disease, there is evidence in favor of the latter, as healthy animals
60 transplanted with feces from those with obesity, colitis or colorectal cancer then go on to develop
61 disease (9–11).

62 In the United States, 1 in 8 women will be diagnosed with breast cancer in her lifetime.
63 While the etiology of breast cancer is still unknown, it is believed to be due to a combination of
64 both genetic and environmental factors. Support for environmental factors comes from migration
65 studies showing an increased incidence of breast cancer amongst migrants and their descendants
66 after they move from a region of low breast cancer risk to a region of high risk (12, 13). Bacterial
67 communities within the host could be one such environmental factor which has not been
68 considered to date.

69 We have previously shown that a breast tissue microbiome exists in a cohort of Canadian
70 and Irish women (14). To determine whether this local microbiome could have a role in
71 modulating the risk of breast cancer development we examined the breast microbiota of 70
72 women who had either breast cancer (normal adjacent tissue collected), benign tumours (normal
73 adjacent tissue collected) or were disease free. Bacteria isolated from cancer patients were
74 characterized and examined for their ability to induce DNA damage.

75

Methods

Microbiome analysis

Tissue collection and processing

Fresh breast tissue was collected from 71 women (aged 19 to 90) undergoing breast surgery at St. Joseph's Hospital in London, Ontario, Canada. Ethical approval was obtained from Western Research Ethics Board and Lawson Health Research Institute, London, Ontario, Canada. Subjects provided written consent for sample collection and subsequent analyses. Fifty-eight women underwent lumpectomies or mastectomies for either benign (n=13) or cancerous (n=45) tumours, and 23 were free of disease and underwent either breast reductions or enhancements. For those women with tumours, the tissue obtained for analysis was collected outside the marginal zone, approximately 5 cm away from the tumour. None of the subjects had been on antibiotics for at least 3 months prior to collection.

After excision, fresh tissue was immediately placed in a sterile vial on ice and homogenized within 30 min of collection. As an environmental control, a tube filled with 1ml of sterile phosphate-buffered saline (PBS) was left open for the duration of the surgical procedure and then processed in parallel with the tissue samples. As an added control, a skin swab was collected of the disinfected breast area prior to surgery. The swab was placed in 1ml of sterile PBS and then vortexed at full speed for 5min to pellet the contents of the swab. The swab was then removed and the liquid stored at −80°C until DNA extraction.

Tissue samples were homogenized in sterile PBS using a PolyTron 2100 homogenizer at 28,000 rpm. The amount of PBS added was based on the weight of the tissue in order to obtain a final concentration of 0.4 g/ml. The homogenate was then stored at −80°C until DNA extraction.

DNA isolation

After tissue homogenates, in sealed containers, were thawed on ice, 400µl (equivalent to 160 mg of tissue) was added to tubes containing 1.2 ml of ASL buffer (QIAamp DNA stool kit; Qiagen) and 400 mg of 0.1-mm-diameter zirconium-glass beads (BioSpec Products). 800µl of the PBS control and 800µl of the skin swab control was also added to tubes containing ASL buffer and beads. Mechanical and chemical lyses were performed on all samples by bead beating at 4,800 rpm for 60s at room temperature and then 60s on ice (repeated twice) (Mini-Beadbeater-1; BioSpec Products), after which the suspension was incubated at 95°C for 5 min. Subsequent procedures were performed using the Qiagen QIAamp DNA stool kit according to the manufacturer's protocol, with the exception of the last step, in which the column was eluted with 120µl of elution buffer. DNA was stored at −20°C until further use.

V6 16S rRNA gene sequencing

PCR amplification

The genomic DNA isolated from the clinical samples was amplified using barcoded primers that amplify the V6 hypervariable region of the 16S rRNA gene (70 base pairs long):

V6-Forward:
5'ACACTCTTTCCCTACACGACGCTCTTCCGATCTnnnn(8)CWACGCGARGAACCTTACC 3'

V6-Reverse:
5'CGGTCTCGGCATTCCTGCTGAACCGCTCTTCCGATCTnnnn(8)ACRACACGAGCTGACGAC 3'

nnnn indicates 4 randomly incorporated nucleotides and "8" represents a specific sample barcode sequence. The PCR was carried out in a 42µl reaction containing 2µl of DNA template (or nuclease-free water as a negative control), 0.15 µg/µl bovine serum albumin, 20µl of 2x GoTaq hot start colorless master mix (Promega) and 10µl of each primer (initial concentration:

3.2pmol/µl). Thermal cycling was carried out in an Eppendorf Mastercyler under the following conditions: initial denaturation at 95°C for 2 minutes followed by 25 cycles of 95°C for 1 minute, 55°C for 1 minute and 72°C for 1 minute. After amplification, the DNA concentration was measured with the Qubit® 2.0 Fluorometer (Invitrogen) using the broad range assay. Equimolar amounts of each PCR product were then pooled together and purified using the QIAquick PCR purification kit (QIAGEN). The pooled PCR purified sample was then paired-end sequenced on the Illumina Mi-Seq platform using a 150 cycle kit with a 2x80 run at the London Regional Genomics Center, London, Ontario, Canada following standard operating procedures.

Sequence processing and taxonomic assignment

Custom Perl and Bash scripts were used to de-multiplex the reads and assign barcoded reads to individual samples. Multiple layers of filtering were employed: (i) Paired end sequences were overlapped with Pandaseq, allowing 0 mismatches in the overlapped reads; (ii) Reads were kept if the sequence included a perfect match to the V6 16S rRNA gene primers; (iii) Barcodes were 8mers with an edit distance of >4 and reads were kept if the sequence were a perfect match to the barcode; (iv) Reads were clustered by 97% identity into operational taxonomic units (OTUs) using the Uclust algorithm of USEARCH v7 (15) which has a *de novo* chimera filter built into it; (v) All singleton OTUs were discarded and those that represented ≥2% of the reads in at least one sample were kept (a filter for PCR and environmental controls and the skin swabs). Taxonomic assignments for each OTU were made by extracting the best hits from the SILVA database (16) and then manually verified using the Ribosomal Database Project (RDP) SeqMatch tool (rdp.cme.msu.edu) and by BLAST against the Green genes database (greengenes.lbl.gov) Taxonomy was assigned based on hits with the highest percentage identities and coverage. If multiple hits fulfilled this criterion, classification was re-assigned to a higher common taxonomy.

147 Data analysis

148 PCoA plots of weighted UniFrac distances (17) were generated in QIIME (18) by using a
149 tree of OTU sequences built with FASTTREE (19) based on an OTU sequence alignment made
150 with MUSCLE (20). PERMANOVA was used to test for statistical significance between groups
151 using 10000 permutations (QIIME package).

152 Microbiome data are compositional in nature (i.e. proportional distributions that are not
153 independent of each other) and thus has several limitations (21). A simple example is as follows:
154 If a sample has two organisms A (50%) and B (50%) and after antibiotic treatment organism A is
155 completely killed, the proportion of B in that sample will now be 100% even if its actual
156 abundance has not changed. Transforming the data, using centered log-ratios (CLR) alleviates
157 the constraints inherent with compositional data (22) by allowing for subcomposition coherence,
158 linear sample independence and normalization of read counts. CLR transformed data with a
159 uniform prior of 0.5 applied was used when generating the K-means clusterplot and the
160 dendogram of Euclidian distances.

161 The ALDEx R package version 2 (21) was used to compare the relative abundance of
162 genera. Values reported in this manuscript represent the expected values of 128 Dirichlet Monte-
163 Carlo instances of CLR transformed data. A value of zero indicates that organism abundance is
164 equal to the geometric mean abundance. Thus, organisms more abundant than the mean will have
165 positive values and those less abundant than the mean will have negative values. Base 2 was used
166 for the logarithm so differences between values represent fold changes. Significance was based
167 on the Benjamini-Hochberg corrected p-value of the Wilcoxon rank test (significance threshold
168 p-val < 0.1)

169 The Microbiome Regression-based Kernel Association Test (MiRKAT) (23) was
170 performed in R using the MiRKAT package. Differences in microbiota profiles were tested using

a kernel metric constructed from weighted UniFrac, unweighted UniFrac and GUniFrac(24) distances and the Bray-Curtis dissimilarity metric. "Optimal" MiRKAT allows for the simultaneous examination of multiple distance/dissimilarity metrics alleviating the problem of choosing the best one and was performed on the aforementioned metrics. The p-values generated were the mean of 128 Dirichlet Monte-Carlo instances.

The R script of "SourceTracker "(version 0.9.1) was used to assess contamination of the tissue microbiota. Tissue samples were designated as "sink" and PBS controls as "source."

Barplots, boxplots, K-means clusterplots and dendograms were all generated in R (http://www.R-project.org/).

Full details regarding Irish tissue sample collection, patient demographics, DNA extraction protocols and the steps followed to generate the OTU table used for the analysis in Supplementary Figure S4 can be found in our previous publications (14, 25)

DNA damage assay

Bacterial strains

Isolates were obtained by plating 100µl of tissue homogenate (normal adjacent tissue and healthy tissue from Canadian subjects) on Columbia blood (CBA), MacConkey and Beef Heart Infusion (BHI) agar plates and incubating both aerobically or anaerobically at 37^{o}C. DNA from single colonies was extracted using the InstaGene Matrix (Bio-Rad) and then amplified using the eubacterial primers pA/pH, which amplifies the complete 16S rRNA gene: pA 5' AGAGTTTGATCCTGGCTCAG 3' pH 5' AAGGAGGTGATCCAGCCGCA 3'

The PCR reaction was carried out in 50µl reaction containing 10µl of DNA template (or nuclease free water as a negative control), 1.5mM $MgCl_2$, 1.0µM of each primer, 0.2mM dNTP, 5µl 10X PCR buffer (Invitrogen), and 0.05 Taq Polymerase (Invitrogen). Thermal cycling was carried out in an Eppendorf Mastercyler under the following conditions: Initial denaturation step at 95^{o}C for

2min, followed by 30 cycles of 94°C for 30s, 55°C for 30s and 72°C for 1min. A final elongation step was performed at 72°C for 10min. 40µl of the PCR mixture was then purified using the QIAquick PCR purification kit (Qiagen) and the purified products sent for Sanger sequencing to the London Regional Genomics Centre, London, Ontario, Canada. Sequences were analyzed using the GenBank 16S ribosomal RNA sequences database and the Greengenes database. Taxonomy was assigned based on the highest Max score. Because the 16S rRNA gene does not differentiate members of the *Enterobacteriaceae* family very well, to confirm that our isolates were indeed *E.coli*, we utilized the API® 20E strip to differentiate species that are part of the this family. *E.coli* strain IHE3034 was kindly provided by Jean Philippe Nougayrède (INRA, Toulouse, France).

Infection assay

HeLa cells were maintained and passaged in DMEM/glutamax media (Invitrogen) supplemented with 10% FBS (Invitrogen). On the day of the experiment a 24 well plate containing sterile cover slips was seeded with 0.5ml of $1x10^5$ cells/ml, resulting in $5x10^4$ HeLa cells/well. The plates were then incubated at 37°C with 5% CO_2 for 24 hours after which times the media was removed and the wells washed with sterile PBS. HeLa cells (2 wells for each organism) were then infected at a MOI 100 for 4 hours with either *Staphylococcus epidermidis* (subject 31), *Micrococcus luteus* (subject 8), *Micrococcus sp* (subject 8), *E.coli* (subject 41 (isolates H and E), subject 34 and strain IHE3034), *Propionibacterium acnes* (subject 20) and *P. granulosum* (subject 20) or at a MOI 1 for 2 hours with *Bacillus cereus* (subject 34 & subject 6). A MOI of 1 was used for *B. cereus* (for 2 hours) instead of 100 (for 4 hours), as used for the other strains, because this was the highest MOI and longest incubation that the HeLa cells could tolerate without dying. The bacterial cultures for infection were prepared by inoculating 5ml of

BHI with 1 colony and incubating aerobically at 37°C for 15 hours, with the exception of *Propionibacterium,* which was incubated anaerobically for 72hr. Bacterial cultures were then spun down at 3500g for 10min, washed and resuspended in PBS. Bacterial cells were then diluted to the appropriate concentration in DMEM media containing 10% FBS and 25mM HEPES. 40µM etoposide (Sigma) was used as a technical positive control. The pH was checked at the end of the experiment to ensure consistency between wells.

Immunofluorescence

After infection, media was removed and HeLa cells were washed 3x with sterile PBS. Cells were then fixed and permeabilized for 12min at room temperature (RT) with a -20°C solution of 95% methanol and 5% acetic acid. Cells were then blocked for an hour with 0.3% Triton-100/5% goat serum. After blocking, a 1/200 dilution of the primary antibody (rabbit anti phospho-H2AX mAb; Cell Signaling technologies) was added and incubated over night at 4°C. After washing a 1/1000 dilution of the secondary antibody (goat anti-rabbit IgG, Alexa Fluor 647 conjugate; Cell Signaling technologies) was added and incubated at RT for 30min. Cells were then counter stained with 1µg/ml of DAPI (Life Technologies) for 1min. Cover slips were mounted on microscope slides containing a drop of ProLong Gold antifade mountant (Life Technologies). The experiments were performed three times.

Images were captured using the NIKON eclipse TE2000-S digital microscope. Eight fields of view for each replicate were recorded, for a total of 16 fields of view for each condition. Using ImageJ software (version 1.48a), the mean fluorescent intensity of each γH2AX stained cell was measured from the digital images. The digital images were also used to determine the percent of total cells stained positive for γH2AX. This was calculated by dividing the number of

red cells (i.e. γH2AX positive) by the number of blue cells (i.e. DAPI stained) and multiplying by one hundred.

Statistics for DNA damage assay

Bar graphs of the mean and standard deviation from the 3 experiments were plotted using Prism (version 5.0a). Significance ($p<0.05$) was tested by a 1 way ANOVA followed by the Dunnet's post hoc test using Prism (version 5.0a)

Results

Microbiota analysis

16S rRNA amplicon sequencing of the V6 hypervariable region was performed on 70 tissue samples and 38 environmental controls. A full summary of patient demographics can be found in **Supplementary Table S1**. To assess the contribution of environmental contamination towards the overall tissue microbiota, we utilized the contamination predictor tool, "SourceTracker", which compared the microbial population in the tissue samples to that of the phosphate buffered saline (PBS) environmental controls that were processed alongside the tissue samples. **Supplementary Fig. S1** shows that while there is contamination present, it makes up only a small proportion (average 10%) of the overall microbial community in breast tissue. A dendogram of Euclidian distances of the centered log-ratio (clr) transformed dataset (22) was then constructed to visualize which tissue samples were similar to the PBS controls and to skin swabs collected from the disinfected breast area prior to surgery. As seen in **Supplementary Fig. S2**, skin swabs, PBS controls and the no template PCR control (NTC) formed a single cluster, which was separate from most of the tissue samples, indicating distinct microbial profiles. To ensure stringent quality control, we removed those tissue samples (27 of them) that were part of the PBS/skin/NTC group from further analysis (**Supplementary Table S2**). In addition, OTUs

present in over 2% abundance in the NTC and PBS controls (11 of them) were also removed from further analysis (**Supplementary Table S2)**. 16S rRNA gene sequencing data of the remaining samples and OTUs, showed a diverse population of bacteria consisting of 61 OTUs and 28 genera (**Fig. 1A**) dominated by the phyla *Proteobacteria* and *Firmicutes* (**Fig. 1B**).

A comparison of normal adjacent tissue from women with breast cancer with that of tissue from healthy women showed distinctly different bacterial profiles on weighted UniFrac PCoA plots (**Fig. 2A**). The PERMANOVA test performed on the dataset showed that the observed differences were statistically significant (10000 permutations; pseudo F-statistic=14.4; p-value <0.01). Unsupervised K-means clustering of the clr transformed dataset indicated two clusters and the PCA plot in **Figure 2B** shows clear separation between the healthy and cancer groups. Differences between the groups were further confirmed using the Microbiome Regression-based Kernel Association Test (MiRKAT) (**Table 1**).

ALDEx2, which allows for the direct comparison of bacterial taxa between groups showed significantly higher compositional abundances of *Prevotella*, *Lactococcus*, *Streptococcus* *Corynebacterium* and *Micrococcus* in healthy patients and *Bacillus*, *Staphylococcus*, *Enterobacteriaceae* (unclassified), *Comamondaceae* (unclassified*)* and *Bacteroidetes* (unclassified) in cancer patients **(Fig. 3) (Supplementary Table S3)**

To assess whether bacteria surrounding the tumour microenvironment might be associated with the severity of cancer, we compared bacterial profiles in normal adjacent tissue from women with various stages of breast cancer. No differences were found based on invasiveness or stage (**Supplementary Fig. S3**). However normal adjacent tissue from women with benign tumours had profiles that were more similar to normal adjacent tissue of women with cancerous tumours rather than tissue from healthy subjects (**Supplementary Table S4**). It is important to note that

no differences were observed between tissue samples collected by different surgeons and/or from different surgical rooms

We have previously published two reports showing which bacteria are present in tumour tissue and normal adjacent tissue of women from Ireland (14, 25). In this report, we now show, using weighted UniFrac distances, that bacterial communities do not differ between tumour tissue and normal adjacent tissue, both at the population level (**Supplementary Fig. S4A**) and within an individual (**Supplementary Fig. S4B**). Thus, when suitably-collected tumour tissue for microbiome analysis is not available, normal adjacent tissue may be a practical alternative.

Assessment of DNA damage ability of breast tissue isolates

E.coli strains belonging to the B2 phylotype harbour the *pks* pathogenicity island, which encodes for machinery for the production of the genotoxin, colibactin. These *pks* + strains have been implicated in colon cancer (26, 27) via its ability to induce DNA double stranded breaks and chromosomal instability (28, 29). As shown in Figure 3, the family *Enterobacteriaceae*, of which *E.coli* is a member, was relatively more abundant in cancer patients compared to healthy controls. For this reason, we wanted to examine whether *E. coli,* cultured from normal adjacent tissue of breast cancer patients, had the ability to induce DNA double stranded breaks (DSB). Cellular levels of γH2AX, a surrogate marker of DSB, were measured in HeLa cells after incubation with various *E.coli* tissue isolates. *E.coli* IHE3034, which contains the pks pathogenicity island and induces DSB (28) was used for comparison.

HeLa cells exposed to *E.coli* tissue isolates had significantly higher levels of γH2AX compared with untreated cells, as measured by mean fluorescent intensity (MFI) and % of cells that stained positive for γH2AX, with levels equivalent to that induced by *E.coli* IHE3034 (**Figure 4**). Additional isolates from breast cancer patients were also examined for the ability to

induce DNA damage; (i) *Bacillus* and *Staphylococcus* were tested as these genera were more abundant in cancer patients; (ii) *Micrococcus*, as this genus was higher in healthy individuals and (iii) *Propionibacterium* as there were no differences in relative abundances between cancer patients and healthy controls. Neither *Bacillus*, *Micrococcus* nor *Propionibacterium* isolates induced DSB, whereas *Staphylococcus* did (**Supplementary Fig. S5**).

γH2AX foci can occur and be resolved very quickly in response to DNA damage, thus a time course was performed, with *Bacillus* treated cells analyzed every 15min over a 2 hour period. No statistically significant differences at any time point were observed between treated and untreated cells (data not shown).

Discussion

This study has shown that different bacterial profiles exist in "normal adjacent" breast tissue from women with breast cancer compared with "normal" tissue from healthy controls. In colorectal cancer (CRC) and oral squamous cell carcinoma (OSCC) bacterial profiles in the stool and saliva respectively, also differ between healthy and diseased patients (30–32) with evidence suggesting that changes in this community composition and function may be driving cancer progression at these sites (33, 34). This raises the possibility that the differences observed in the breast could also play a role in breast cancer progression. We acknowledge that the average age differed between the two groups with the cancer cohort having a mean and median age of 62 and the healthy cohort having a mean age of 49 and a median age of 53. Considering that the mean and median age of the benign group was 38 and 36 respectively and the microbial profiles did not differ between the benign and cancer groups, we don't believe that the difference observed between the healthy and cancer group were due to difference in ages. Menopausal status does not appear to be a factor either since no differences in microbial profiles were observed between pre

and post menopausal women in the healthy cohort and pre and post menopausal women with either benign or cancerous tumours.

Enterobacteriaceae and *Staphylococcus* are two taxa found in higher abundance in breast cancer patients compared with healthy controls. Examination of three *E.coli* isolates (a member of the *Enterobacteriaceae* family) and one *Staphylococcus epidermidis* isolate, cultured from normal adjacent tissue of breast cancer patients, all displayed the ability to induce DNA double stranded breaks (DSB). DSB are the most detrimental type of DNA damage and are caused by genotoxins, reactive oxygen species, and ionizing radiation(35). Non-homologous end joining (NHEJ), the mechanism by which DSB are repaired, is extremely error- prone often resulting in missing bases at the site of damage (35). Accumulation of these mis-repairs within the cell over time leads to genomic instability and eventually cancer (36). DSB caused by bacteria such as *Helicobacter pylori* and certain strains of *E.coli* have been shown to induce chromosomal instability with prolonged exposure (29, 37). While the same mechanisms may be involved in the *in vitro* assay described here (or indeed breast tissue transformation), further tests would need to be done to verify whether chromosomal abnormalities do occur subsequent to the DNA damage induced by these breast isolates. In support of this hypothesis, total cell numbers were consistent between all treated and untreated groups, suggesting no induction of apoptosis. It is important to note that bacterial induced DNA damage may not be sufficient in itself to promote breast cancer development unless it occurs in a genetically susceptible host. All genetic and 3-30% of sporadic cancer cases have mutations in DNA repair or DNA checkpoint machinery (38). Thus women who have impaired DNA repair/checkpoints may be more susceptible to bacterial induced DNA damage and may be at a higher risk of developing breast cancer than women without these mutations, even if they have the same "detrimental" microbes in their mammary glands.

356 *Bacillus* was also elevated in breast cancer patients compared with healthy controls,
357 confirming our previous findings (14). While *Bacillus* did not induce DSB like *E.coli* and
358 *S.epidermidis* it could have other pro-carcinogenic effects. One study has shown that a *Bacillus*
359 *cereus* strain, isolated from gingival plaque, metabolizes the hormone progesterone into 5 alpha-
360 pregnane-3,20-dione (5αP) (39). 5αP is higher in breast tumours compared with healthy breast
361 tissue (40) and is believed to promote tumour development by stimulating cell proliferation (40,
362 41). While our molecular analysis did not permit species level identification, all *Bacillus* strains
363 cultured from our breast cancer patients were of the species *B.cereus.*
364 An epidemiological study has shown that women who drink fermented milk products
365 have a reduced risk of breast cancer development, irrespective of multivariable risk factors (42).
366 This protection could be attributed to the health promoting properties of the various lactic acid
367 bacteria (LAB) present in fermented products. *Lactococccus* and *Streptococcus*, two such
368 bacteria that were higher in healthy women compared with breast cancer patients, exhibit anti-
369 carcinogenic properties and could play a role in prevention. Natural killer (NK) cells are vital in
370 controlling tumour growth with epidemiological studies showing that low NK cell activity (from
371 peripheral blood mononuclear cells (PBMC)) is associated with an increased incidence of breast
372 cancer (43, 44). *Lactococcus lactis* has been shown to activate murine splenic NK cells,
373 enhancing cellular immunity (45). While no studies have yet been published comparing NK cell
374 functionality in the breast between "normal" (i.e. healthy patients) and "normal adjacent" (breast
375 cancer patients) tissue, it could be assumed, based on the PBMC data, that NK functionality is
376 also impaired in the breast of those with cancer. *Lactococcus sp* present in the mammary glands,
377 could be modulating cellular immunity by maintaining the cytotoxic activity of resident NK cells
378 (46) thus helping to prevent cancer development. *Streptococcus thermophilus* on the other hand,

379 better than any other LAB tested, protects against DNA damage caused by reactive oxygen
380 species by producing antioxidant metabolites that neutralize peroxide and superoxide radicals
381 (47).

382 Orally administered *Lactobacillus sp*, has shown to be protective in animal models of
383 breast cancer (48). While total numbers did not differ between healthy and diseased patients,
384 those with breast cancer may not experience the full anti-carcinogenic benefits afforded by
385 *Lactobacillus* due to the decrease in *Lactococcus* and *Streptococcus*, as LAB have been shown to
386 act in synergy with each other (49).

387 *Prevotella*, which was more abundant in healthy women compared with breast cancer
388 patients, produces the short chain fatty acid (SCFA), propionate. Propionate, like other SCFA,
389 has many beneficial health effects in the gut, one of them being the ability to regulate colorectal
390 tumour growth (50). In both animal and human studies, higher levels of *Prevotella* were observed
391 in the stool of healthy subjects compared to those with CRC (10, 30). However in the oral cavity,
392 patients with OSCC have higher levels of *Prevotella* compared with healthy controls and when
393 *Prevotella* presence was used as a diagnostic tool, the authors could predict 80% of the cancer
394 cases (32). The conflicting association of *Prevotella* between CRC and OSCC could be due to the
395 fact that metabolites function differently at different body sites. While SCFA are anti-
396 inflammatory in the colon and associated with health (51), in the vagina, they are pro-
397 inflammatory and associated with bacterial vaginosis (52). What role *Prevotella* and/or
398 propionate may be playing in breast health (or disease) remains to be determined.

399 It is interesting that the microbiome profile of normal adjacent tissue from women with
400 benign tumours was similar to that of normal adjacent tissue from cancer patients, rather than
401 normal tissue from healthy women and raises the question as to why these women with benign
402 tumours do not have cancer, if we believe there could be a link between bacteria and breast

cancer. In women with benign disease, DNA damage caused by bacteria could be responsible for enhanced cellular proliferation leading to tumour formation, similar to what may be occurring in cancer patients, however, other factors that could promote transformation and malignancy of this tumour is reduced in these women compared to those with cancer. One of these factors could be the increased secretion of pro-angiogenic and/or inflammatory molecules from immune and epithelial cells in women who have cancer. Another possibility is that women with benign tumours have lower levels of DNA damaging bacteria then those with cancerous tumours, lowering the probability of multiple onco-genic genes becoming mutated. Further studies following healthy women and those with benign tumours for development of breast cancer could shed more light on which bacterial strains could be driving cancer development.

While we have reported differential abundances of certain organisms between health and diseased states, in reality, it is probably not a single organism driving disease progression or protection but rather an interplay of poly-microbial interactions. To get a better understanding of the microbial influence on breast cancer, the functionality of these microbes should be investigated. Further studies examining bacterial metabolites and bacterial-induced host metabolites would provide vital information on the role of bacteria in breast health.

Conclusion

This study has shown that bacterial profiles differ in breast tissue between healthy subjects and normal adjacent tissue of breast cancer patients. Some of the bacteria that were relatively more abundant in breast cancer patients had the ability to induce DNA double stranded breaks. Further studies need to be done to examine whether this DNA damage can lead to chromosomal aberrations and whether the differences in the bacterial profiles are a cause or a consequence of the disease. This study raises important questions as to the role of the breast

Applied and Environmental Microbiology

microbiota in breast cancer development or prevention and whether bacteria could be harnessed for interventions to help prevent disease onset.

Acknowledgements

We would like to thank all the women who provided tissue samples for the study. In addition, members of the Gloor lab for fruitful discussions on 16S rRNA gene sequencing analysis; Dr. Robert Richards and all the clinical and administrative staff at St Joseph's Hospital for their support throughout the study. We are also very grateful to Jean Philippe Nougayrède (INRA, Toulouse, France) for providing us with *E.coli* strain IHE3034 and for his insight and help with our DNA damage assay.

Author contributions

CU designed the study, recruited subjects, collected and prepared the samples for microbial analysis, analyzed 16S rRNA sequencing data, performed and analyzed the DNA damage assay and wrote the manuscript. GG provided co-supervision and input into microbiome acquisition and analysis and manuscript review. MB helped with study design, provided input into data collection and analysis, collected tissue from tumour patients and reviewed the manuscript. LS helped with study design and collected tissue from tumour patients. MT supervised the collection of tissue samples from women in Ireland, provided input into data interpretation and reviewed the manuscript. GR conceptualized the study, helped with study design and manuscript writing, supervised data collection and analysis and provided financial support.

Financial support: CU was supported by (i) CIHR Strategic Training Program in Cancer Research and Technology Transfer scholarship and (ii) Translational Breast Cancer Research Studentship.

References

1. **Darveau RP**. 2010. Periodontitis: a polymicrobial disruption of host homeostasis. Nat. Rev. Microbiol. **8**:481–90.

2. **Ximénez-Fyvie LA, Haffajee AD, Socransky SS**. 2000. Comparison of the microbiota of supra- and subgingival plaque in health and periodontitis. J. Clin. Periodontol. **27**:648–57.

3. **Frank DN, St Amand AL, Feldman RA, Boedeker EC, Harpaz N, Pace NR**. 2007. Molecular-phylogenetic characterization of microbial community imbalances in human inflammatory bowel diseases. Proc. Natl. Acad. Sci. U. S. A. **104**:13780–5.

4. **Gao Z, Tseng C, Strober BE, Pei Z, Blaser MJ**. 2008. Substantial alterations of the cutaneous bacterial biota in psoriatic lesions. PLoS One **3**:e2719.

5. **Hilty M, Burke C, Pedro H, Cardenas P, Bush A, Bossley C, Davies J, Ervine A, Poulter L, Pachter L, Moffatt MF, Cookson WOC**. 2010. Disordered microbial communities in asthmatic airways. PLoS One **5**:e8578.

6. **Larsen N, Vogensen FK, van den Berg FWJ, Nielsen DS, Andreasen AS, Pedersen BK, Al-Soud WA, Sørensen SJ, Hansen LH, Jakobsen M**. 2010. Gut microbiota in human adults with type 2 diabetes differs from non-diabetic adults. PLoS One **5**:e9085.

7. **Hummelen R, Fernandes AD, Macklaim JM, Dickson RJ, Changalucha J, Gloor GB, Reid G**. 2010. Deep sequencing of the vaginal microbiota of women with HIV. PLoS One **5**:e12078.

8. **Mira-Pascual L, Cabrera-Rubio R, Ocon S, Costales P, Parra A, Suarez A, Moris F, Rodrigo L, Mira A, Collado MC**. 2014. Microbial mucosal colonic shifts associated with the development of colorectal cancer reveal the presence of different bacterial and archaeal biomarkers. J. Gastroenterol. **50**:167–179.

9. **Garrett WS, Lord GM, Punit S, Lugo-Villarino G, Mazmanian SK, Ito S, Glickman JN, Glimcher LH**. 2007. Communicable ulcerative colitis induced by T-bet deficiency in the innate immune system. Cell **131**:33–45.

10. **Zackular JP, Baxter NT, Iverson KD, Sadler WD, Petrosino JF, Chen GY, Schloss PD**. 2013. The gut microbiome modulates colon tumorigenesis. MBio **4**:e00692–13.

11. **Turnbaugh PJ, Hamady M, Yatsunenko T, Cantarel BL, Duncan A, Ley RE, Sogin ML, Jones WJ, Roe BA, Affourtit JP, Egholm M, Henrissat B, Heath AC, Knight R, Gordon JI**. 2009. A core gut microbiome in obese and lean twins. Nature **457**:480–4.

12. **Le GM, Gomez SL, Clarke CA, Glaser SL, West DW**. 2002. Cancer incidence patterns among Vietnamese in the United States and Ha Noi, Vietnam. Int. J. Cancer **102**:412–7.

13. **Shimizu H, Ross RK, Bernstein L, Yatani R, Henderson BE, Mack TM**. 1991. Cancers of the prostate and breast among Japanese and white immigrants in Los Angeles County. Br. J. Cancer **63**:963–6.

14. **Urbaniak C, Cummins J, Brackstone M, Macklaim JM, Gloor GB, Baban CK, Scott L, O'Hanlon DM, Burton JP, Francis KP, Tangney M, Reid G**. 2014. Microbiota of human breast tissue. Appl. Environ. Microbiol. **80**:3007–14.

15. **Edgar RC**. 2010. Search and clustering orders of magnitude faster than BLAST. Bioinformatics **26**:2460–1.

16. **Pruesse E, Quast C, Knittel K, Fuchs BM, Ludwig W, Peplies J, Glöckner FO**. 2007. SILVA: a comprehensive online resource for quality checked and aligned ribosomal RNA sequence data compatible with ARB. Nucleic Acids Res. **35**:7188–96.

17. **Lozupone C, Knight R**. 2005. UniFrac: a new phylogenetic method for comparing microbial communities. Appl. Environ. Microbiol. **71**:8228–35.

18. **Caporaso JG, Kuczynski J, Stombaugh J, Bittinger K, Bushman FD, Costello EK, Fierer N, Peña AG, Goodrich JK, Gordon JI, Huttley GA, Kelley ST, Knights D, Koenig JE, Ley RE, Lozupone CA, McDonald D, Muegge BD, Pirrung M, Reeder J, Sevinsky JR, Turnbaugh PJ, Walters WA, Widmann J, Yatsunenko T, Zaneveld J, Knight R**. 2010. QIIME allows analysis of high-throughput community sequencing data. Nat. Methods **7**:335–6.

19. **Price MN, Dehal PS, Arkin AP**. 2009. FastTree: computing large minimum evolution trees with profiles instead of a distance matrix. Mol. Biol. Evol. **26**:1641–50.

20. **Edgar RC**. 2004. MUSCLE: a multiple sequence alignment method with reduced time and space complexity. BMC Bioinformatics **5**:113.

21. **Fernandes AD, Reid JN, Macklaim JM, McMurrough TA, Edgell DR, Gloor GB**. 2014. Unifying the analysis of high-throughput sequencing datasets: characterizing RNA-seq, 16S rRNA gene sequencing and selective growth experiments by compositional data analysis. Microbiome **2**:15.

22. **Aitchison J**. 1986. The Statistical Analysis of Compositional Data. Chapman & Hall, London, England.

23. **Zhao N, Chen J, Carroll IM, Ringel-Kulka T, Epstein MP, Zhou H, Zhou JJ, Ringel Y, Li H, Wu MC**. 2015. Testing in Microbiome-Profiling Studies with MiRKAT, the Microbiome Regression-Based Kernel Association Test. Am. J. Hum. Genet. **96**:797–807.

24. **Chen J, Bittinger K, Charlson ES, Hoffmann C, Lewis J, Wu GD, Collman RG, Bushman FD, Li H**. 2012. Associating microbiome composition with environmental covariates using generalized UniFrac distances. Bioinformatics **28**:2106–13.

25. **Lehouritis P, Cummins J, Stanton M, Murphy CT, McCarthy FO, Reid G, Urbaniak C, Byrne WL, Tangney M**. 2015. Local bacteria affect the efficacy of chemotherapeutic drugs. Sci. Rep. **5**:14554.

26. **Arthur JC, Perez-Chanona E, Mühlbauer M, Tomkovich S, Uronis JM, Fan T-J, Campbell BJ, Abujamel T, Dogan B, Rogers AB, Rhodes JM, Stintzi A, Simpson KW, Hansen JJ, Keku TO, Fodor AA, Jobin C**. 2012. Intestinal inflammation targets cancer-inducing activity of the microbiota. Science **338**:120–3.

27. **Buc E, Dubois D, Sauvanet P, Raisch J, Delmas J, Darfeuille-Michaud A, Pezet D, Bonnet R**. 2013. High prevalence of mucosa-associated E. coli producing cyclomodulin and genotoxin in colon cancer. PLoS One **8**:e56964.

28. **Nougayrède J-P, Homburg S, Taieb F, Boury M, Brzuszkiewicz E, Gottschalk G, Buchrieser C, Hacker J, Dobrindt U, Oswald E**. 2006. Escherichia coli induces DNA double-strand breaks in eukaryotic cells. Science **313**:848–51.

29. **Cuevas-Ramos G, Petit CR, Marcq I, Boury M, Oswald E, Nougayrède J-P**. 2010. Escherichia coli induces DNA damage in vivo and triggers genomic instability in mammalian cells. Proc. Natl. Acad. Sci. U. S. A. **107**:11537–42.

30. **Weir TL, Manter DK, Sheflin AM, Barnett BA, Heuberger AL, Ryan EP**. 2013. Stool microbiome and metabolome differences between colorectal cancer patients and healthy adults. PLoS One **8**:e70803.

31. **Wang T, Cai G, Qiu Y, Fei N, Zhang M, Pang X, Jia W, Cai S, Zhao L**. 2012. Structural segregation of gut microbiota between colorectal cancer patients and healthy volunteers. ISME J. **6**:320–9.

32. **Mager DL, Haffajee AD, Devlin PM, Norris CM, Posner MR, Goodson JM**. 2005. The salivary microbiota as a diagnostic indicator of oral cancer: a descriptive, non-randomized study of cancer-free and oral squamous cell carcinoma subjects. J. Transl. Med. **3**:27.

33. **Schwabe RF, Jobin C**. 2013. The microbiome and cancer. Nat. Rev. Cancer **13**:800–12.

34. **Ahn J, Chen CY, Hayes RB**. 2012. Oral microbiome and oral and gastrointestinal cancer risk. Cancer Causes Control **23**:399–404.

35. **Lees-Miller S**. 2003. Repair of DNA double strand breaks by non-homologous end joining. Biochimie **85**:1161–1173.

36. **Khanna KK, Jackson SP**. 2001. DNA double-strand breaks: signaling, repair and the cancer connection. Nat. Genet. **27**:247–54.

37. **Toller IM, Neelsen KJ, Steger M, Hartung ML, Hottiger MO, Stucki M, Kalali B, Gerhard M, Sartori AA, Lopes M, Müller A**. 2011. Carcinogenic bacterial pathogen

Helicobacter pylori triggers DNA double-strand breaks and a DNA damage response in its host cells. Proc. Natl. Acad. Sci. U. S. A. **108**:14944–9.

38. **Negrini S, Gorgoulis VG, Halazonetis TD**. 2010. Genomic instability--an evolving hallmark of cancer. Nat. Rev. Mol. Cell Biol. **11**:220–8.

39. **Ojanotko-Harri A, Nikkari T, Harri MP, Paunio KU**. 1990. Metabolism of progesterone and testosterone by Bacillus cereus strain Socransky 67 and Streptococcus mutans strain Ingbritt. Oral Microbiol. Immunol. **5**:237–9.

40. **Wiebe JP, Muzia D, Hu J, Szwajcer D, Hill SA, Seachrist JL**. 2000. The 4-pregnene and 5alpha-pregnane progesterone metabolites formed in nontumorous and tumorous breast tissue have opposite effects on breast cell proliferation and adhesion. Cancer Res. **60**:936–43.

41. **Wiebe JP**. 2006. Progesterone metabolites in breast cancer. Endocr. Relat. Cancer **13**:717–38.

42. **van't Veer P, Dekker JM, Lamers JW, Kok FJ, Schouten EG, Brants HA, Sturmans F, Hermus RJ**. 1989. Consumption of fermented milk products and breast cancer: a case-control study in The Netherlands. Cancer Res. **49**:4020–3.

43. **Imai K, Matsuyama S, Miyake S, Suga K, Nakachi K**. 2000. Natural cytotoxic activity of peripheral-blood lymphocytes and cancer incidence: an 11-year follow-up study of a general population. Lancet **356**:1795–9.

44. **Strayer DR, Carter WA, Mayberry SD, Pequignot E, Brodsky I**. 1984. Low natural cytotoxicity of peripheral blood mononuclear cells in individuals with high familial incidences of cancer. Cancer Res. **44**:370–4.

45. **Kosaka A, Yan H, Ohashi S, Gotoh Y, Sato A, Tsutsui H, Kaisho T, Toda T, Tsuji NM**. 2012. Lactococcus lactis subsp. cremoris FC triggers IFN-γ production from NK and T cells via IL-12 and IL-18. Int. Immunopharmacol. **14**:729–33.

46. **Carrega P, Bonaccorsi I, Di Carlo E, Morandi B, Paul P, Rizzello V, Cipollone G, Navarra G, Mingari MC, Moretta L, Ferlazzo G**. 2014. CD56(bright)perforin(low) noncytotoxic human NK cells are abundant in both healthy and neoplastic solid tissues and recirculate to secondary lymphoid organs via afferent lymph. J. Immunol. **192**:3805–15.

47. **Koller VJ, Marian B, Stidl R, Nersesyan A, Winter H, Simić T, Sontag G, Knasmüller S**. 2008. Impact of lactic acid bacteria on oxidative DNA damage in human derived colon cells. Food Chem. Toxicol. **46**:1221–1229.

48. **De Moreno de LeBlanc A, Matar C, Thériault C, Perdigón G**. 2005. Effects of milk fermented by Lactobacillus helveticus R389 on immune cells associated to mammary glands in normal and a breast cancer model. Immunobiology **210**:349–58.

587 49. **Shiou S-R, Yu Y, Guo Y, He S-M, Mziray-Andrew CH, Hoenig J, Sun J, Petrof EO, Claud EC**. 2013. Synergistic protection of combined probiotic conditioned media against
589 neonatal necrotizing enterocolitis-like intestinal injury. PLoS One **8**:e65108.

590 50. **Hosseini E, Grootaert C, Verstraete W, Van de Wiele T**. 2011. Propionate as a health-
591 promoting microbial metabolite in the human gut. Nutr. Rev. **69**:245–58.

592 51. **Louis P, Hold GL, Flint HJ**. 2014. The gut microbiota, bacterial metabolites and
593 colorectal cancer. Nat. Rev. Microbiol. **12**:661–672.

594 52. **Aldunate M, Srbinovski D, Hearps AC, Latham CF, Ramsland PA, Gugasyan R, Cone RA, Tachedjian G**. 2015. Antimicrobial and immune modulatory effects of lactic
596 acid and short chain fatty acids produced by vaginal microbiota associated with eubiosis
597 and bacterial vaginosis. Front. Physiol. **6**:164.

598

599

600 **Figure captions**

601 **Figure 1: Breast tissue microbiota in 43 Canadian women identified by 16S rRNA amplicon**
602 **sequencing.** (A) The relative abundances of bacterial genera in different breast tissue samples
603 were visualized by bar plots. Each bar represents a subject and each colored box a bacterial
604 taxon. The height of a coloured box represents the relative abundance of that organism within the
605 sample. Taxa present in less than 2% abundance in a given sample are displayed in the
606 "Remaining fraction" at the top of the graph (gray boxes). As shown by the bar plots, a variety of
607 bacteria were detected in breast tissue. The legend is read from bottom to top, with the bottom
608 organism on the legend corresponding to the bottom colored box on the bar plot. (B) Box plots of
609 the six phyla identified in breast tissue. The box signifies the 75% (upper) and 25% (lower)
610 quartiles and thus shows where 50% of the samples lie. The black line inside the box represents
611 the median. The whiskers represent the lowest datum still within 1.5 interquartile range (IQR) of
612 the lower quartile and the highest datum still within 1.5 IQR of the upper quartile. Outliers are
613 shown with open circles.

614 **Figure 2: Comparison of bacterial profiles between breast cancer patients and healthy**
615 **controls.** (A) Weighted UniFrac principal coordinate (PCoA) plot and (B) K-means clusterplot of
616 centered log-ratio transformed data. Each breast tissue sample, represented by a coloured point is
617 plotted on a three-dimensional, 3-axis plane representing 79% of the variation observed between
618 all samples (A) or 44.85% of the variation on a 2-axis plane (B). Samples (points) that cluster
619 together are similar in biota composition and abundance. The distinct separation between the two
620 groups indicates that bacterial profiles differ between women with and without cancer. The
621 PERMANOVA test performed on the weighted UniFrac distances showed that the observed
622 differences were statistically significant (10000 permutations; pseudo F-statistic=14.4; p-value
623 <0.01)
624
625
626 **Figure 3: Differences in relative abundances of taxa exist between healthy and cancer**
627 **patients.** The top panel shows the bacteria that had statistically significant higher relative
628 abundances in healthy patients compared to those with cancer (i.e. normal adjacent tissue) and
629 the bottom panel shows the bacteria that had statistically significant higher relative abundances in
630 cancer patients compared to healthy controls. The box signifies the 75% (upper) and 25% (lower)
631 quartiles and thus shows where 50% of the samples lie. The black line inside the box represents
632 the median. The whiskers represent the lowest datum still within 1.5 interquartile range (IQR) of
633 the lower quartile and the highest datum still within 1.5 IQR of the upper quartile. Outliers are
634 shown with open circles. Significance was based on the Benjamini-Hochberg corrected p-value
635 of the Wilcoxon rank test (significance threshold p-val < 0.1).
636

637 **Figure 4: DNA damage ability of *E.coli* isolated from breast cancer patients.** *E.coli* was
638 isolated from normal adjacent tissue of 2 patients with breast cancer and tested for its ability to
639 induce DNA double stranded breaks. *E.coli* (isolates H and E) from subject 41, isolate L from
640 subject 34 and strain IHE3034 were incubated with HeLa cells at MOI 100 for 4hr and then
641 stained for γH2AX and DAPI. Etoposide, a chemical that induces DNA double stranded breaks in
642 eukaryotic cells, was used as a technical positive control. (A) Representative immunofluorescent
643 images of HeLa cells at 1000x magnification. (B) Image J was used to measure the mean
644 fluorescent intensity (MFI) of γH2AX positive cells from the digitally acquired images. (C)
645 Percent of total cells stained for γH2AX calculated from the immunofluorescent images. Data
646 displayed in the bar graphs represent the mean +/- SD of 3 experiments representing a total of 48
647 fields of view and approximately 300 cells for each treatment group. ** denotes p-value <0.01
648
649
650

Fig. 1A

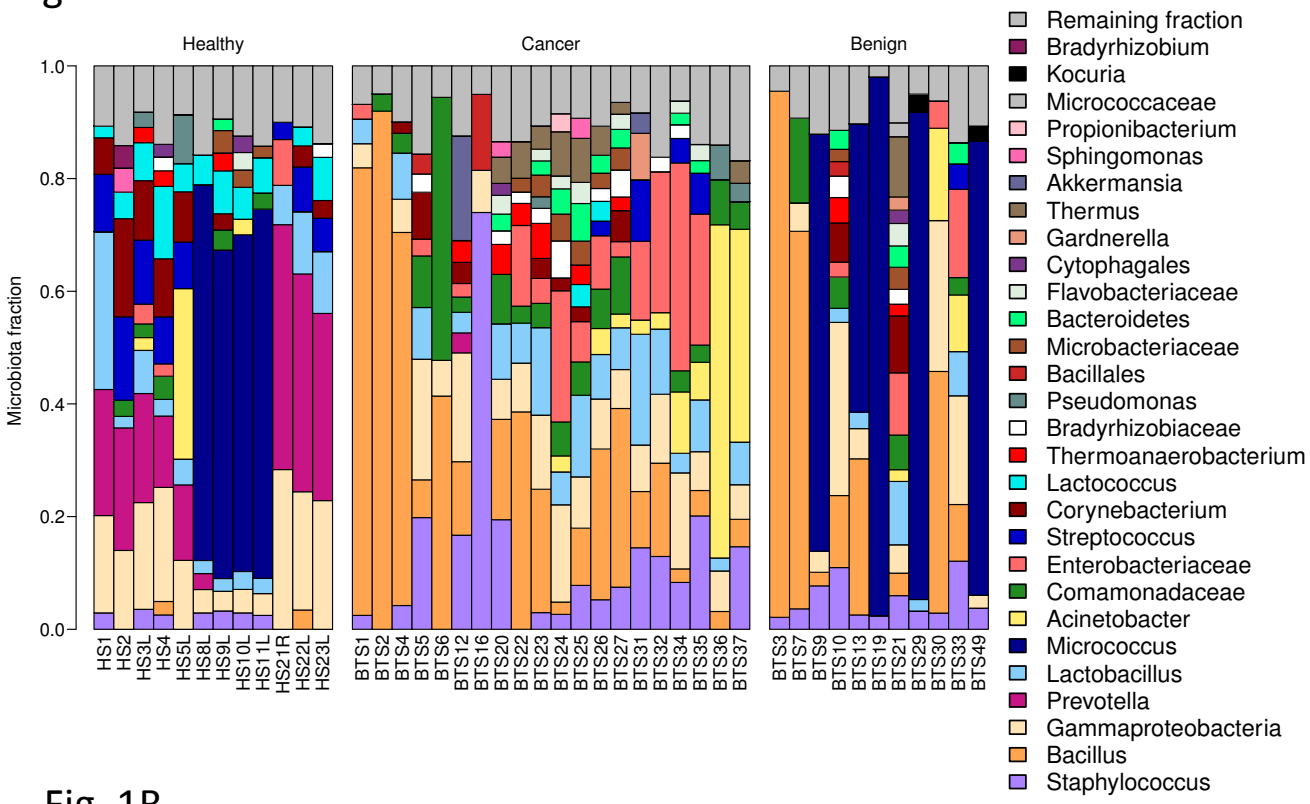

Fig. 1B

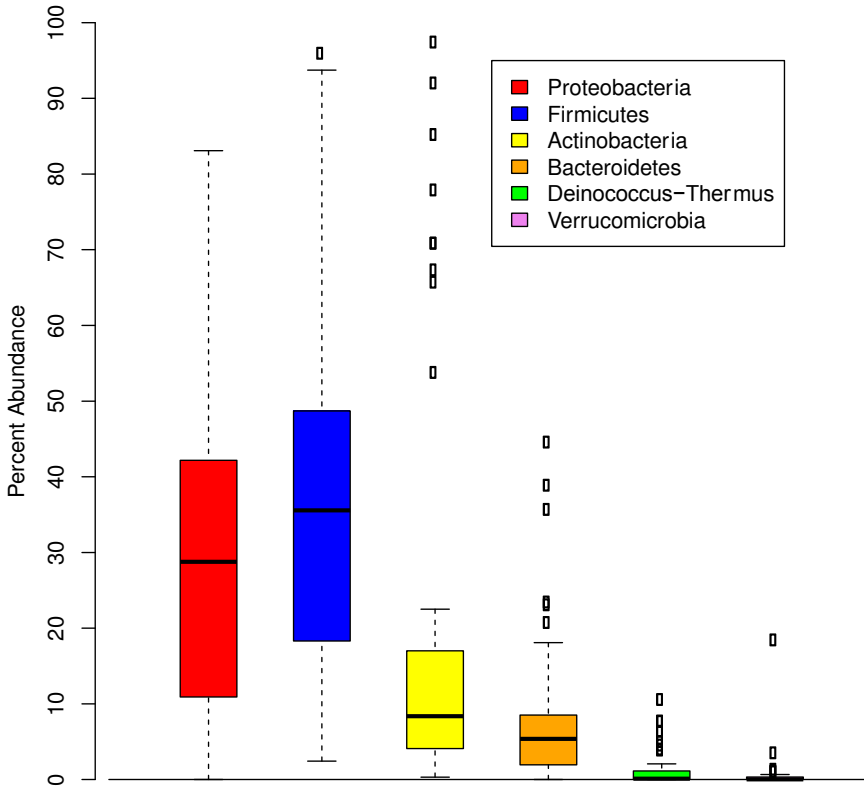

Fig. 2A

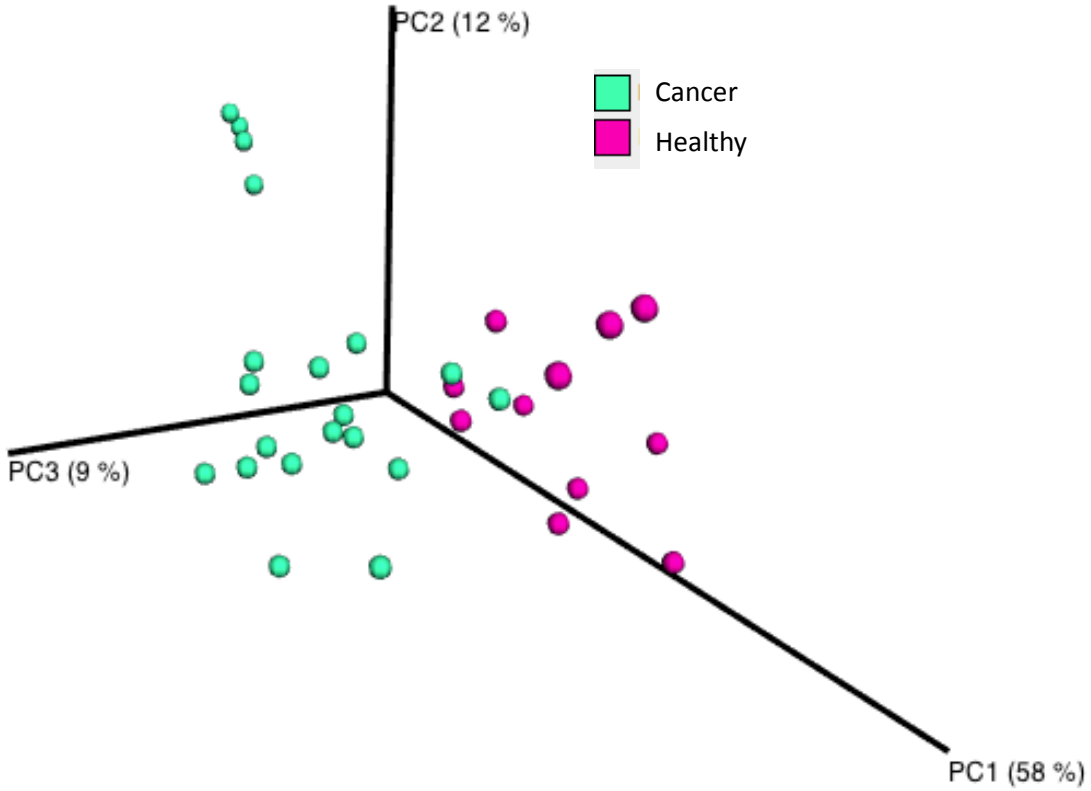

Fig. 2B

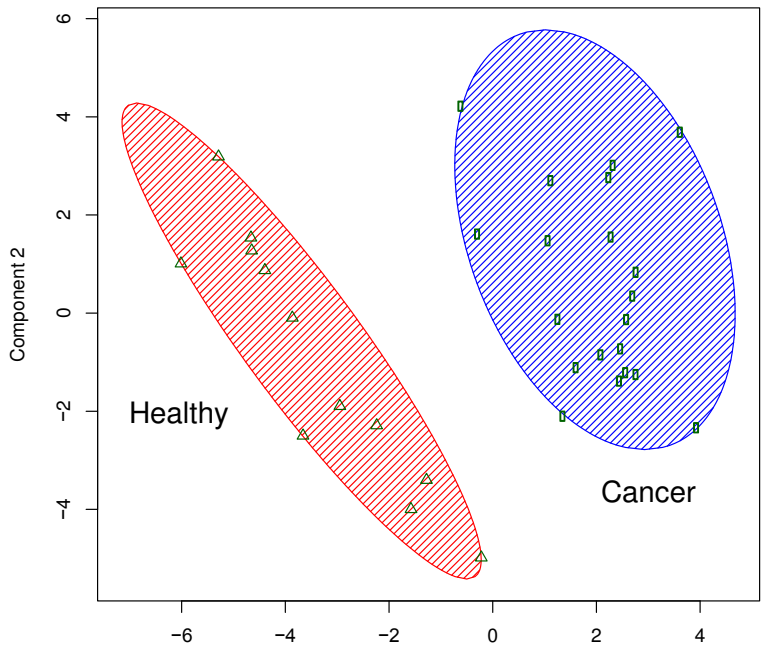

Fig. 3

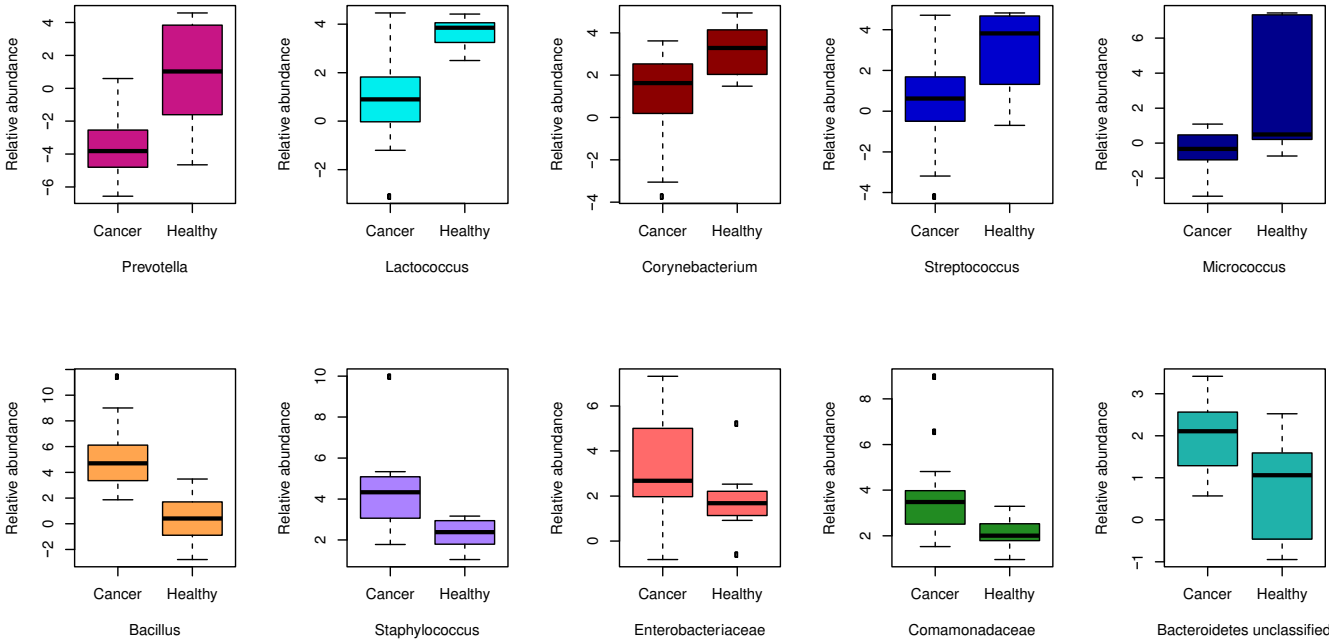

Fig. 4A

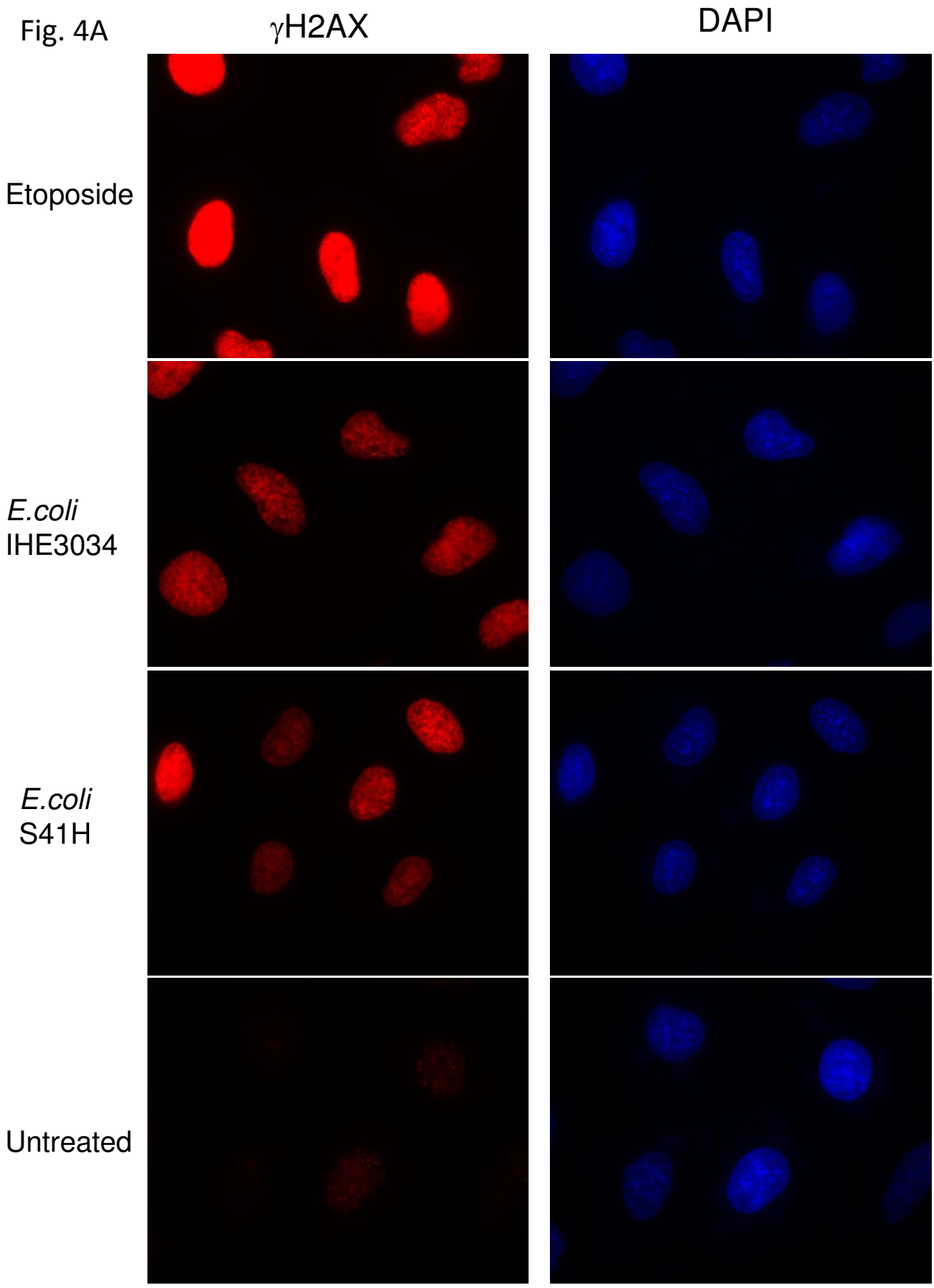

Fig 4B

Fig 4C

Table 1: Summary of p-values generated by MIRKAT.
p-values displayed represent the min, max, average and median values generated from 128 Dirichlet Monte-Carlo instances for each of the 4 distance-based metrics shown (columns 2-5). "Optimal" refers to the p-values obtained when the 4 distance-based metrics are analyzed simultaneously.

	Bray-Curtis	Weighted UniFrac	Unweighted UniFrac	GUniFrac α=0.5	Optimal
Min	4.58E-05	2.64E-06	4.12E-06	2.64E-06	0
Max	0.000129826	1.04E-05	0.004191322	1.15E-05	0
Average	7.87E-05	4.52E-06	0.000395004	5.33E-06	0
Median	7.70E-05	4.24E-06	2.05E-04	4.87E-06	0